Characteristics of Binary Tropical Cyclones Observed in the Western North Pacific for 62 Years (1951–2012)

WOOK JANG AND HYE-YEONG CHUN

Department of Atmospheric Sciences, Yonsei University, Seoul, South Korea

(Manuscript received 8 October 2014, in final form 11 January 2015)

ABSTRACT

The statistical and dynamical characteristics of binary tropical cyclones (TCs) observed in the western North Pacific (WNP) for 62 years (1951–2012) are investigated by using best track and reanalysis data. A total of 98 binary TCs occurred with an annual average of 1.58. The occurrence frequency of binary TCs shows significant year-to-year variations and there are two peaks in the mid-1960s and early 1990s. Three-fourths (76.3%) of the binary TCs occurred between July and September, which is consistent with the high activity season of TCs in general. A relatively higher track density for binary TCs is present to the east of the maximum track density for total TCs. This result is likely due to the differences in the locations of genesis and environmental steering flow between binary and total TCs. The poleward steering flow, weaker vertical wind shear, and warmer sea surface temperature are pronounced for binary TCs, and these result in a longer lifetime of TCs, which can increase the chances that they would be detected as binary TCs. By applying the clustering analysis technique, six representative trajectories of the binary TCs are obtained. The transitional speed and recurving location are significantly different with respect to the clustered types. The trajectories of each type are strongly related to the temporal variations in the environmental steering flow and the location of the North Pacific high.

1. Introduction

The interaction of two or more tropical cyclones (TCs) is one of the primary sources of error when forecasting TCs (Brand 1970, hereafter B70; Jarrell et al. 1978; Neumann 1981; Prieto et al. 2003). A number of modeling and observational studies have been performed in order to investigate the interaction of binary TCs, since it was first suggested by Fujiwhara's (1921, 1923, 1931) tank experiments. The modeling studies can be categorized into two types: idealized and real-case simulations. In previous studies that used idealized simulations with a nondivergent barotropic model, the critical separation distance for the merger of two TCs and the factors determining the attraction or repulsion of two vortices were investigated (DeMaria and Chan 1984; Pokhil et al. 1990; Ritchie and Holland 1993; Shin et al. 2006). In a three-dimensional framework, which is influenced by baroclinicity, the interactions of two idealized vortices are more complicated and the characteristics of the interactions are different from those in the barotropic model (Chang 1983; Falkovich et al. 1995; Khain et al. 2000). In real-case studies, the interactions of binary TCs have been investigated by analyzing the simulation results from mesoscale numerical models in various methods, such as the potential vorticity inversion technique (Yang et al. 2008), the vortex removal technique (Wu et al. 2012), and the diagnosis of interaction regimes (Jang and Chun 2013).

Several observational studies have been conducted in order to investigate the characteristics of binary TCs in the western North Pacific (WNP) using various methods and data, because binary TCs in the WNP have drawn more attention because of that region having the world's strongest TC activity. Among those studies, B70, Dong and Neumann (1983, hereafter DN83), and Wu et al. (2011, hereafter W11) investigated the statistical and dynamical characteristics of binary TCs in the WNP by using objective criteria based on the best track data for detecting binary TCs. B70 showed that the mutual

Denotes Open Access content.

Corresponding author address: Dr. Hye-Yeong Chun, Department of Atmospheric Sciences, Yonsei University, 262 Seongsanno, Seodaemun-ku, Seoul 120-749, South Korea.
E-mail: chunhy@yonsei.ac.kr

DOI: 10.1175/MWR-D-14-00331.1

interaction between two TCs becomes clear when the separation distance is approximately 1400 km and slight attractions between two TCs are shown when the separation distance is less than 740 km. DN83 found that most binary TCs in the WNP showed cyclonic rotation relative to a counterpart TC and they suggested that the *Fujiwhara effect* becomes dominant by exceeding the influence of the flow in the intertropical convergence zone when the separation distance is less than 650 km. In W11, based on the yearly and monthly distributions of binary TCs in the WNP, they proposed seven distinct types of binary TC tracks by using a clustering analysis technique and they showed the strong relationship between the representative tracks of binary TCs and steering flow.

Unlike the aforementioned three studies that applied certain criteria to the detection of binary TCs, some observational studies selected binary TCs subjectively based on their movements. By selecting 10 binary TCs with clear mutual interaction, Lander and Holland (1993) found that the classical Fujiwhara model is rarely applicable to the real atmosphere and a sequence of interactions was found including capturing, cyclonic orbiting, and merging or escaping. Based on the best track data between 1989 and 1995, Carr et al. (1997) proposed three conceptual modes (direct, semidirect, and indirect TC interaction) to describe binary TC interactions observed in the WNP. The three modes are distinct by the degree of interaction and the relationship between TCs and subtropical anticyclones. Carr and Elsberry (1998) suggested two criteria—separation distance and rotation rate—to categorize observed binary TCs into three conceptual modes, which can explain approximately 80% of binary TCs that occurred in the WNP between 1986 and 1996.

There have also been observational studies about binary TCs that are based on satellite images or analysis data rather than best track data (e.g., Kuo et al. 2000; Prieto et al. 2003; Wu et al. 2003). By using a series of satellite images, Kuo et al. (2000) classified the interaction regimes between Typhoons Zeb and Alex (1998) based on Dritschel and Waugh's (1992) theory. Prieto et al. (2003) investigated the interaction between Hurricane Gil (2001) and Tropical Storm Henriette (2001) by using *GOES-10* visible images. Wu et al. (2003) explained the unusual movements of Tropical Storm Bopha (2000) due to the interaction with Supertyphoon Saomai (2000) by using potential vorticity diagnosis based on analysis data, while Jang and Chun (2013) investigated the effects of topography on the evolution of Typhoon Saomai (2006) under the influence of Tropical Storm Bopha (2006).

In the previous studies (B70, DN83, and W11) that examined the spatiotemporal distribution of binary TCs based on best track data, the intensities of two TCs, their separation distance, and coexistence time were the primary factors used for defining binary TCs. In the criterion for distance, the previous studies detected a binary TC pair when two TCs exist within a certain distance of each other (B70: 1300 km, DN83: 1334 km, W11: 1600 km) at least one time. Considering that the interaction between two TCs occurs sequentially as noted by Lander and Holland (1993), the criterion for distance in the previous studies provided insufficient time for the interaction of two TCs. Therefore, in the present study, a binary TC is defined as when two TCs coexist within 1600 km of each other for more than consecutive 24 h with a maximum wind speed of greater than 17.2 m s^{-1}. We use less strict conditions on the coexistence time, which is defined as the time for the coexistence of two TC pairs without restriction on the distance between the two TCs, than DN83 and W11, because of the rather strict criteria for the distance in the present study. The criteria for binary TC detection in the present study and those in the aforementioned three previous studies are listed in Table 1.

The purpose of this study is to investigate the statistical and dynamical characteristics of binary TCs observed in the WNP and the effects of environmental conditions on binary TCs by using a relatively long period of data (1951–2012). In section 2, the data and methodology used in this study are described. In section 3, the spatiotemporal distribution of binary TCs in the WNP and the influence of environmental conditions are examined. In section 4, the six representative tracks of binary TCs and the effects of steering flow and the North Pacific high on the clustered tracks are shown. In the final section, we summarize the study and provide the conclusions.

2. Data and methodology

a. Data

In this study, the best track data from the Joint Typhoon Warning Center (JTWC) over the WNP between 1951 and 2012 are used. These data include the 6-hourly information of an individual TC, such as the date, time, location, central pressure, and maximum wind speed. To investigate the effects of the North Pacific high, the environmental steering flow, and vertical wind shear on the genesis and propagation of binary TCs, the geopotential height and the zonal and meridional winds from the 6-hourly National Centers for Environmental Prediction–National Center for Atmospheric Research (NCEP–NCAR) reanalysis data with a 2.5° × 2.5° horizontal resolution (Kalnay et al. 1996) are used. The daily mean sea surface temperature (SST) data from the

TABLE 1. Criteria of binary TC detection from B70, DN83, W11, and the present study.

	B70	DN83	W11	Present study
Intensity	$>33.4\,m\,s^{-1}$ at one time	$>18\,m\,s^{-1}$ at one time	$>18\,m\,s^{-1}$ for 48 h	$>18\,m\,s^{-1}$ for 24 h
Distance	<1300 km at one time	<1334 km at one time	<1600 km at one time	<1600 km for 24 h
Coexistence time	>one time	>48 h	>48 h	>24 h
Ocean	Open ocean	None	None	None

National Oceanic and Atmospheric Administration (NOAA) with a $0.25° \times 0.25°$ horizontal resolution from 1982 to 2012 (Reynolds et al. 2007) are used to examine the effects of SST. High-resolution SST data are used to investigate the detailed structure of SST in this study, because SST shows significant latitudinal variation.

b. Methodology

The clustering analysis technique suggested by Gaffney (2004) is used to categorize the tracks of binary TCs in the WNP. (The MATLAB toolbox with detailed information is available online at http://www.datalab.uci.edu/resources/CCT/.) This analysis technique collects the tracks of TCs showing similar patterns, which is widely used in analyzing typical tracks of TCs (e.g., Camargo et al. 2007; Chand and Walsh 2009; W11). To apply the clustering technique to binary TCs, two TCs selected as a binary TC pair are separated into western and eastern TCs. Then the western TCs are clustered into six types and the corresponding eastern TCs are included in each cluster. The results are generally similar when the eastern TCs are clustered first (not shown).

To investigate the environmental conditions for each type of binary TCs selected from the clustering technique, composite analysis is used. The steering flow is calculated by averaging the horizontal wind at all of the levels between 200 and 850 hPa in the WNP (0°–50°N, 100°E–180°), following the same definition as in previous studies (e.g., George and Gray 1976; Chan and Gray 1982; Ho et al. 2009). Note that the steering flow is calculated in this study without excluding TCs in the circulation, although TC circulation should be removed to have true ''environmental steering flow.''

3. Spatiotemporal distribution of binary TCs

a. Temporal variations

According to the definition of a binary TC used in this study, 98 binary systems occurred (among the 1763 total TCs) during a period of 62 years (1951–2012) in the WNP, with an annual average of 1.58. This implies that approximately three TCs per year in the WNP can be categorized as a binary TC on average, which is less than 12% of total TCs. The annual occurrence in the present study is larger than that in B70 (1.02), while it is smaller than that in DN83 (2.24) and W11 (3.87) when the criteria from previous studies are applied to the best track data for the 62 years considered in the present study. The larger annual frequency of binary TCs in the present study in comparison with that in B70, in spite of more strict criterion for the distance condition, is primarily due to less strict intensity condition in this study. When the intensity condition in this study is replaced by that in B70, the annual occurrence decreases from 1.58 to 1.06. The smaller annual occurrence of binary TCs in the present study in comparison with DN83 and W11 is due to the reduced binary TCs in the present study by applying consecutive 24-h duration to two TCs separated by less than 1600 km.

Figure 1a shows the annual variation in the number of total (green bar) and binary TCs (red bar) with the ratio of binary TCs to total TC numbers (black solid line). The occurrence frequency of binary TCs shows significant year-to-year variation and there are two peaks in the mid-1960s and the early 1990s. The correlation coefficient between the number of total and binary TCs is 0.40, which is statistically significant at a 95% confidence level. The power spectrum of the number of total TCs reveals spectral peaks at 3.6 and 2.5 years and that of binary TCs at 5.6 years with a 95% confidence level (not shown). The difference in the spectral peaks and the modest correlation between total and binary TCs shows their unclear relationship.

The peaks of 2.5 and 3.6 years for total TCs are likely associated with the atmospheric interannual variations, such as El Niño–Southern Oscillation (ENSO), quasi-biennial oscillation (QBO), and monsoon activity. Therefore, the number of total and binary TCs that occurred during each phase of the interannual variations is examined by selecting 15 years of each phase of the interannual variations. Following the methodology of Camargo et al. (2007), 15 El Niño and 15 La Niña years are chosen by selecting the 15 years with the highest and the 15 years with the lowest values of the Niño-3.4 index, respectively. Similarly, 15 westerly and 15 easterly phase QBO years are chosen by selecting the 15 largest positive and 15 largest negative differences in the zonal wind between 50 and 70 hPa, respectively (Huesmann and Hitchman 2001; Ho et al. 2009). For monsoon activity, the monsoon index suggested by Wang and Fan (1999)

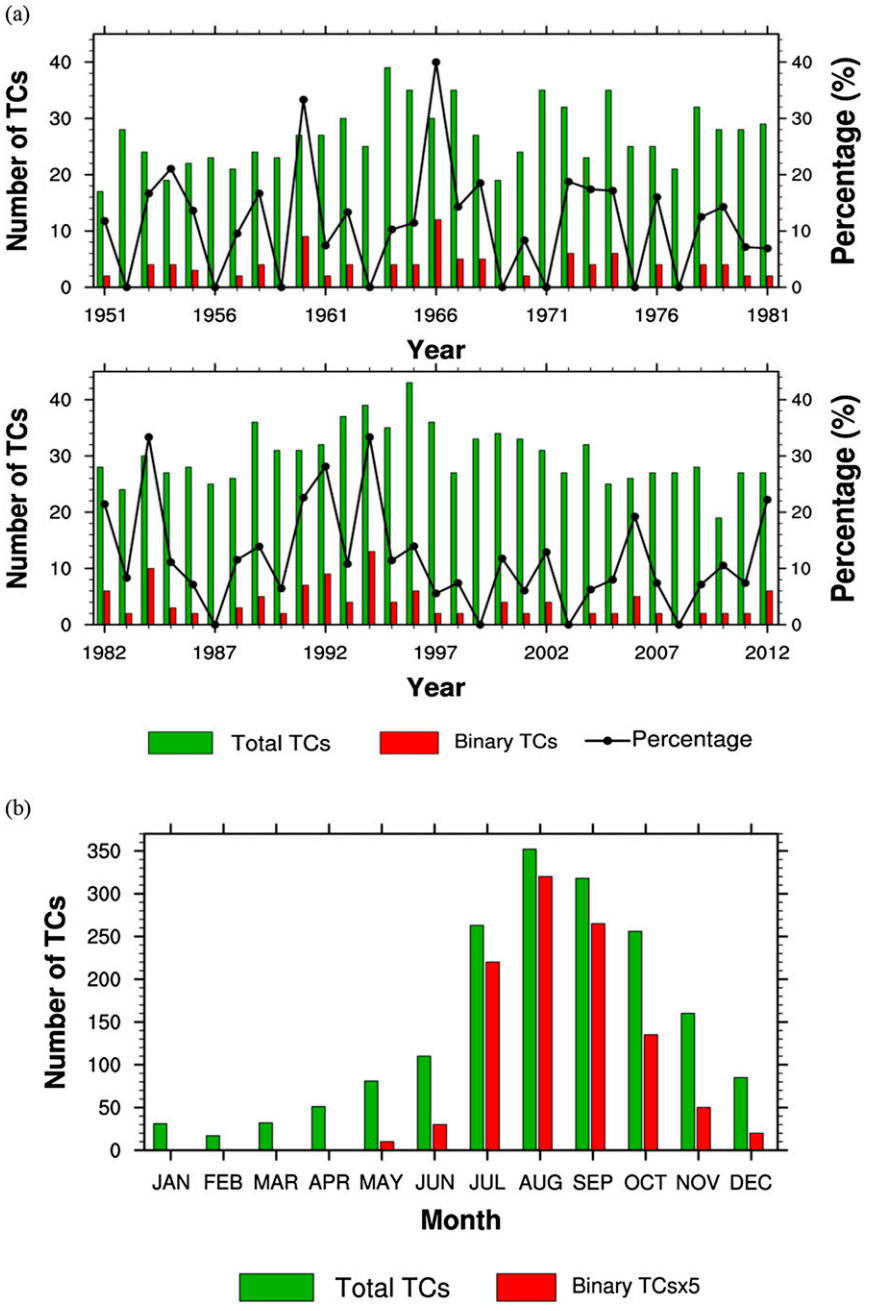

FIG. 1. (a) Annual and (b) monthly variation of the number of total (green bar) and binary (red bar) TCs. Black solid line in (a) indicates the ratio of the number of binary TCs to total TCs. The number of binary TCs in (b) is multiplied by five.

and Wang et al. (2001), which is defined as the difference in the zonal wind at 850 hPa between the South China Sea (5°–15°N, 100°–130°E) and the East China Sea (20°–30°N, 110°–140°E) is calculated, and the 15 strong and the 15 weak monsoon years are chosen by selecting the 15 years of the highest and the 15 years of the lowest values of the monsoon index, respectively. Table 2 shows the number of total and binary TCs that occurred in each phase of the interannual variations. There is no significant difference in the number of total TCs that occurred in the two phases of ENSO (El Niño: 408, La Niña: 407) and QBO (westerly phase: 443, easterly phase: 435). These results are consistent with those of previous studies that showed the unclear relationships

TABLE 2. The number of total and binary TCs that occurred in 15 years of each phase for ENSO, QBO, and monsoon activity. The methodology for selecting the 15 years is described in the text.

	ENSO		QBO		Monsoon	
	El Niño	La Niña	Westerly	Easterly	Strong	Weak
Total TCs	408	407	443	435	459	407
Binary TCs	43	35	48	63	59	44

between the number of total TCs in the WNP and ENSO (Lander 1994) or QBO (Ho et al. 2009). On the other hand, 52 more TCs occurred during the strong monsoon years than the weak monsoon years, and this difference is significant at a 90% confidence level. The occurrence of more TCs in the strong monsoon years are consistent with the results of previous studies, which demonstrated the favorable effects of the strong monsoon trough on the TC genesis frequency in the WNP (Lighthill et al. 1994; McBride 1995).

For binary TCs, 8, 15, and 15 more TCs occurred during the El Niño, easterly phase, and strong monsoon years than the La Niña, westerly phase, and weak monsoon years, respectively. The differences in the ratio of binary to total TCs between the phases are 1.9%, 3.7%, and 2.1% for ENSO, QBO, and monsoon activity, respectively, implying for the largest difference in the ratio by QBO phases. However, the differences in the number of binary TCs between the phases of interannual variations are not statistically significant, likely due to the small number of sampling years. However, the interannual variation in the number of binary TCs is beyond the scope of the current study and it needs to be studied in the future.

Figure 1b shows the monthly distribution of the number of total (green bar) and binary TCs (red bar). Three-fourths of the binary TCs (76.3%) occurred from July to September, which is consistent with the season of high TC genesis. The number of binary TCs is highest in August followed by September and July, which is consistent with total TCs. The ratios of the occurrence frequency of binary TCs to total TCs in July, August, and September are 16.7%, 18.2%, and 16.7%, respectively.

b. Spatial distribution

Figures 2a and 2b show the track density for total and binary TCs, respectively. The track density is defined as the number of TCs that move into a 2.5° × 2.5° (latitude × longitude) grid box. The maximum of track density is present in the east and west sides of the Philippines influenced by the prevailing westerlies and North Pacific high. For binary TCs, a higher track density is present in the east and north of the maximum track density for total TCs. The ratio of the track density of binary TCs to total TCs (Fig. 2c) indicates that the tracks of binary TCs shift to the northeast and eastward of the major regions of the tracks for total TCs, moving toward the Korean Peninsula and Japan. The differences in the spatial distribution of the track densities for total and binary TCs are likely due to the differences in the genesis locations and environmental conditions, which will be shown in the next section. Figures 3a and 3b show the genesis density for total and binary TCs, respectively. Similar to the track density, the genesis density is defined as the number of TCs for which each TC first forms in a 2.5° × 2.5° grid box. A relatively higher genesis density is present in the wide region between 5°–15°N and 115°–150°E for total TCs (Fig. 3a), while it is concentrated in the narrow region between 5°–15°N and 135°–150°E for binary TCs (Fig. 3b). The ratio of the genesis density of binary TCs to total TCs (Fig. 3c) shows that the genesis locations of binary TCs are concentrated to the north of 15°N and to the east of 150°E, which is shifted to the north and east from the genesis location of total TCs. The genesis distribution partly contributes to the differences in the track density between total and binary TCs shown in Fig. 2, because the track of the TC is influenced by its genesis location. In addition, the track density is strongly associated with the environmental conditions as well as genesis location and, therefore, the effects of environmental conditions on binary TCs will be investigated in the following section.

c. Environmental conditions for binary TCs

Figure 4 shows the composites of the geopotential height, steering flow, magnitude of the deep-layer (between 200 and 850 hPa) vertical wind shear, SST, and the differences in them between binary and nonbinary TCs at their genesis time. It should be noted that in the present study, we define the vertical wind shear as the difference in the magnitude of the horizontal wind vector between 200 and 850 hPa (in m s^{-1}). When binary TCs are formed, the center of the North Pacific high is located at 30°N, 165°E, and the anticyclonic steering flow is present near the North Pacific high (Fig. 4a). In comparison to binary TCs, the North Pacific high for nonbinary TCs expands farther to the Philippines and

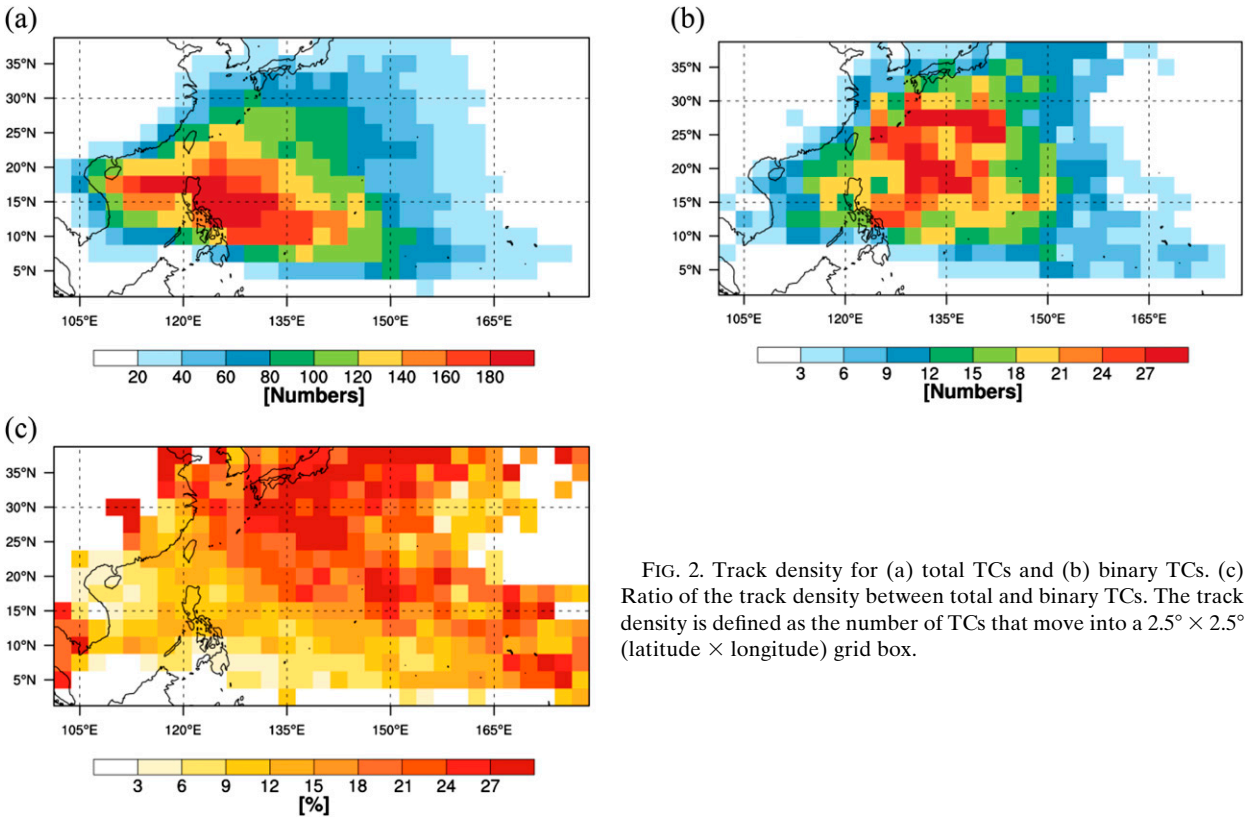

FIG. 2. Track density for (a) total TCs and (b) binary TCs. (c) Ratio of the track density between total and binary TCs. The track density is defined as the number of TCs that move into a 2.5° × 2.5° (latitude × longitude) grid box.

Taiwan, and the related anticyclonic steering flow is also expanded (Fig. 4d). The differences in the geopotential height and the steering flow between binary and nonbinary TCs (Fig. 4g) show statistically significant cyclonic rotations over 10°–20°N and 105°–150°E, and the related poleward steering flow in the eastern end of the cyclonic rotation (10°–20°N, 150°E). This poleward steering flow for binary TCs prevents the westward movements of the TCs and keeps TCs in the ocean, which results in a different spatial distribution of the track density shown in Fig. 2.

The spatial patterns of the vertical wind shear for binary and nonbinary TCs are similar, except that the two maxima are shown to the west of the Korean Peninsula (40°N, 110°E) and to the east of Japan (45°N, 155°E) for binary TCs, while a maximum is in the southeastern part of Japan (40°N, 140°E) for nonbinary TCs. The strength of the vertical wind shear is much smaller in a wide area in the WNP between 20°–40°N and 100°E–180° for binary TCs as shown in Fig. 4h. Considering that the strong vertical wind shear prohibits the intensification of TCs (McBride and Zehr 1981; Merrill 1988; DeMaria 1996; Frank and Ritchie 2001), the weaker vertical wind shear in this region can lead to higher developments of binary TCs, which is evidenced in the relatively high genesis density of binary TCs in this region (Fig. 3c). On the other hand, a stronger vertical wind shear is present in the low-latitude region at 0°–15°N, 100°–160°E for binary TCs than for nonbinary TCs, and this distribution is responsible for the northward shift of the track and genesis densities as shown in Figs. 2 and 3.

The composites of SST are constructed by using the data from 1982 to 2012 at the genesis day of each TC, and the numbers of binary and nonbinary TCs in this period are 112 and 813, respectively. The composites of SST for binary and nonbinary TCs generally show similar spatial distribution with significant latitudinal variation (Figs. 4c and 4f). The SST for binary TCs is significantly larger than that for nonbinary TCs to the north of 20°N and the differences between binary and nonbinary TCs generally increase with latitude in this region (Fig. 4i). The differences to the south of 20°N are not significant except for to the east of 165°E. Considering the positive effects of SST on the intensification of TCs (Emanuel 1988), generally larger SSTs for binary TCs to the north of 20°N are likely to provide favorable conditions for the development of stronger TCs. The differences in SST between binary and nonbinary TCs have similar spatial features when they are calculated

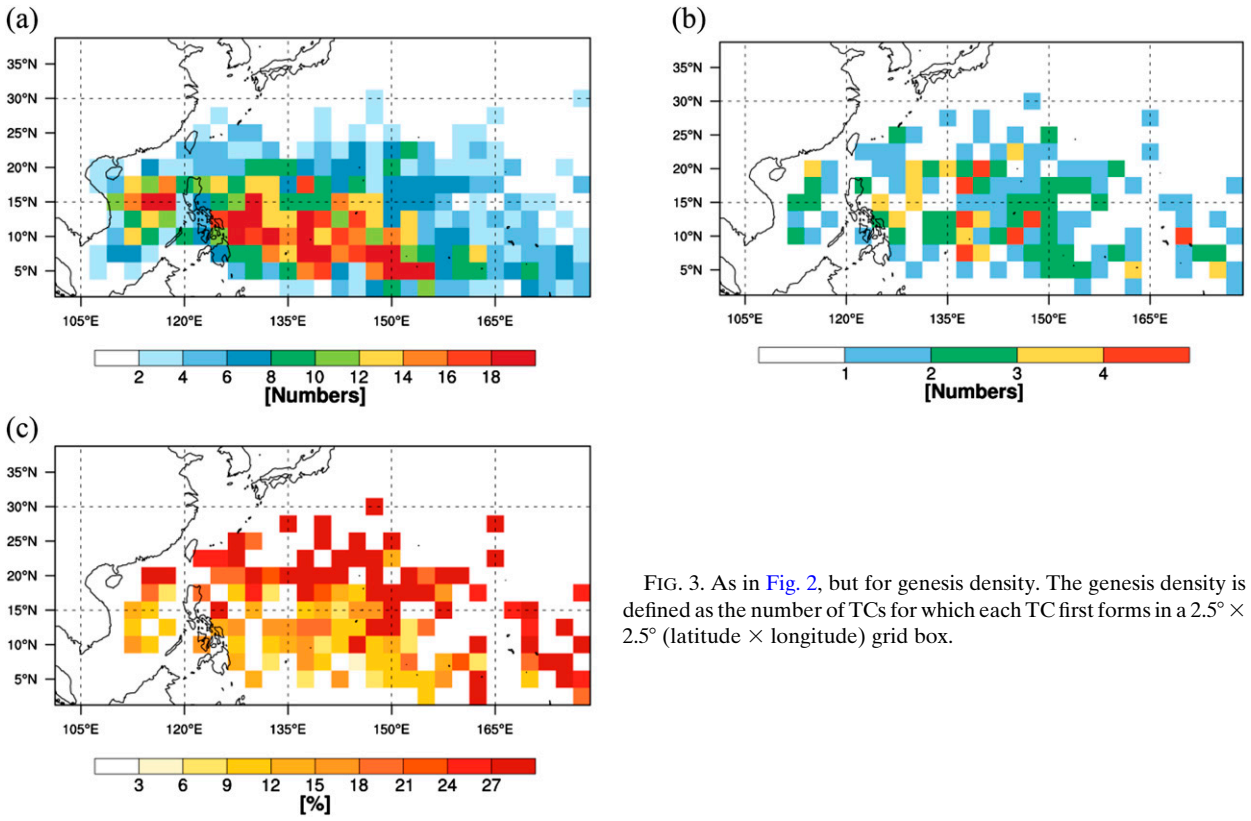

FIG. 3. As in Fig. 2, but for genesis density. The genesis density is defined as the number of TCs for which each TC first forms in a 2.5° × 2.5° (latitude × longitude) grid box.

using the SST data from the NCEP/Department of Energy (DOE) Reanalysis 2 (Kanamitsu et al. 2002) with coarser resolution (T62, 1.875° × 1.915°), except for a smoother feature and slightly wider region for warmer SSTs for binary TCs (not shown).

It should be noted that the intensities of the two TCs, their separation distance, and the coexistence time are used as the criteria for detecting binary TCs. Considering these criteria, long-lived TCs are favorable to be classified into binary TCs, because they have better chances to interact with the preexisting or new TCs. The average lifetime of binary and nonbinary TCs for the entire 62 years considered in the present study is 221.92 and 169.58 h, respectively. The average lifetime of binary TCs is approximately 31% larger than that of nonbinary TCs, and this difference is significant at a 99% confidence level. As shown in Figs. 2 and 4, binary TCs have a relatively higher track density in the ocean and stay longer in the ocean with a warmer SST. This is a favorable condition for long-lived TCs due to the intensification by a continuous supply of water vapor from the ocean. A weaker vertical wind shear in the genesis region of binary TCs also provides favorable condition for TC development and contributes to the evolution of long-lived TCs.

4. Categorization of binary TCs

a. Representative tracks

In this section, tracks of binary TCs observed in the WNP are categorized into six types based on the clustering technique (Gaffney 2004). The clustering analysis is applied to 84 binary cases, after excluding 14 triple TC cases. Figure 5 shows the individual tracks (thin solid lines) belonging to each type and the regressed tracks (thick solid lines with dots) for each type. The regressed tracks are obtained by using a second-order polynomial regression model that minimizes the sum of the deviation between the regressed and observed tracks (Kleinbaum et al. 1997). The red (blue) curves denote the tracks for the western (eastern) TC of a binary TC pair. The number of TCs belonging to the six types, named type A, B, C, D, E, and F, are 8, 21, 11, 17, 16, and 11, respectively. In type A, the western TCs (WTCs) continuously move westward to the Philippines and the eastern TCs (ETCs) move westward or recurve (Fig. 5a). In the regressed tracks of type B, WTCs and ETCs recurve to the west of the Philippines and to the east of Taiwan, respectively (Fig. 5b). In type C, the recurving location of the regressed tracks shift more eastward and the curvatures

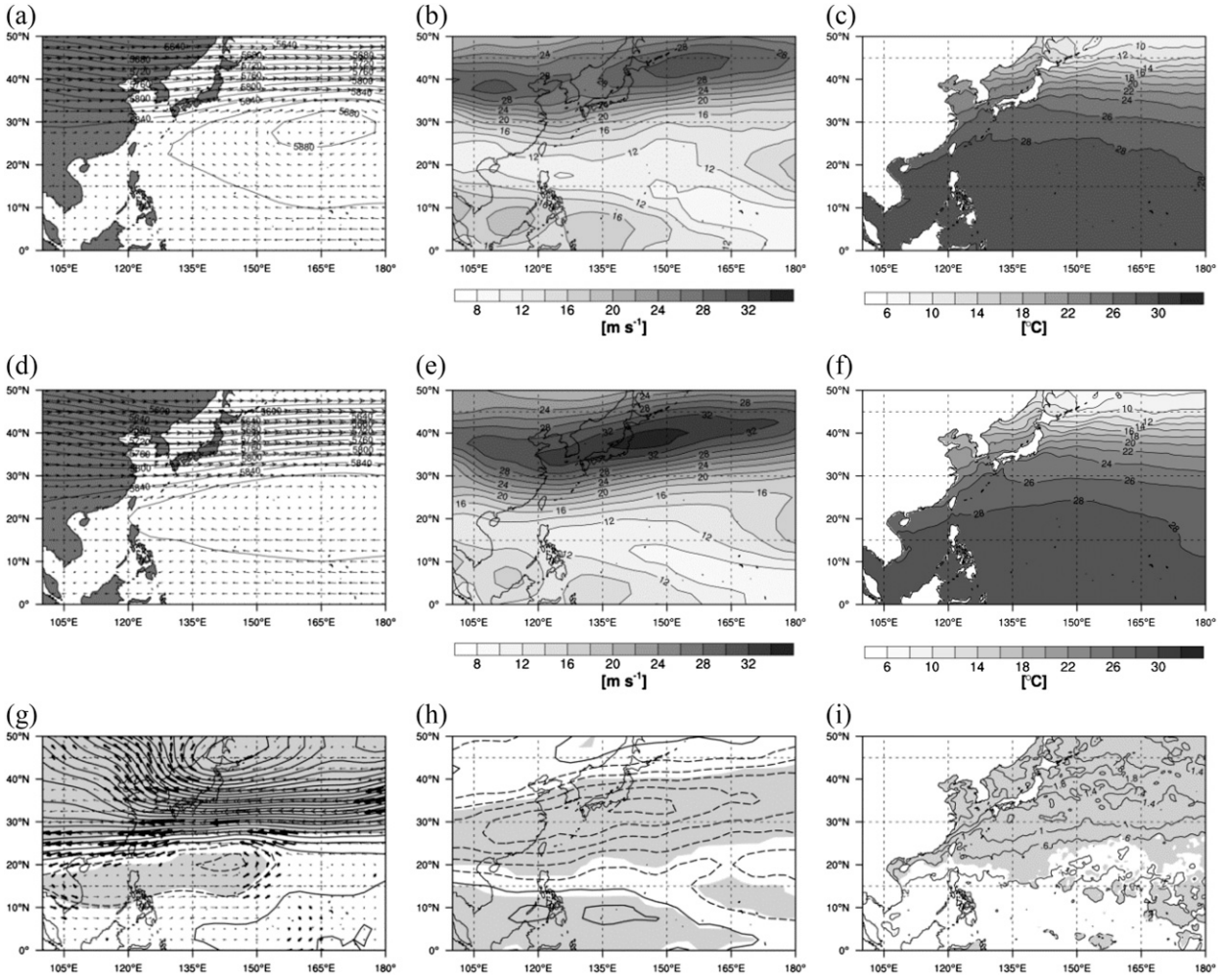

FIG. 4. Composites of the geopotential height at 500 hPa and environmental steering flow for (a) binary and (d) nonbinary TCs. (g) The differences between (a) and (d) are shown. The magnitude of the vertical wind shear between 200 and 850 hPa for (b) binary and (e) nonbinary TCs, and (h) their differences. (c),(f),(i) As in (b),(e),(h), but showing SST. The gray shadings and bold vectors in (g),(h), and (i) indicate significant areas at a 95% confidence level. The contour intervals in (a) and (d) are 20 m, and those in (g) are 4 m. The contours intervals in (b),(e), and (h) are 2 m s^{-1}. The contour intervals in (c) and (f) are 2°C and that in (i) is 0.4°C.

of the tracks are larger than those in type B (Fig. 5c). The regressed tracks of types D, E, and F showed unusual movements in comparison with the general tracks of TCs in the WNP. In type D, WTCs move to the Korean Peninsula or the eastern part of China, and ETCs generally recurve to the south of Japan (Fig. 5d). Two regressed tracks in type E interact for movement to the southeast of Japan (Fig. 5e). The individual tracks in type E are quite divergent from the regressed tracks. In type F, WTCs recurve to the southwest of Japan, while ETCs recurve to the southeast of Japan or move northwestward (Fig. 5f). It is noteworthy that the grouping of each type can be different from the number of clustering, in general. In the present study, we choose six types, because they represent all of the observed tracks with different characteristics, as shown in Fig. 5. W11 categorized binary TCs in the WNP into seven types. Among the seven types from W11, two of the regressed tracks are similar to those of types A and C in the present study and three of them show slightly modified patterns from those of types A, B, and F in the present study. It should be noted that the regressed track with a concentric circle pattern shown in W11 is not present in this study. The different features in the regressed tracks between W11 and the present study are due to the use of different best track data, criteria for detecting binary TC, and clustering numbers. In the following section, we investigate the effects of environmental conditions on the clustered tracks shown in Fig. 5.

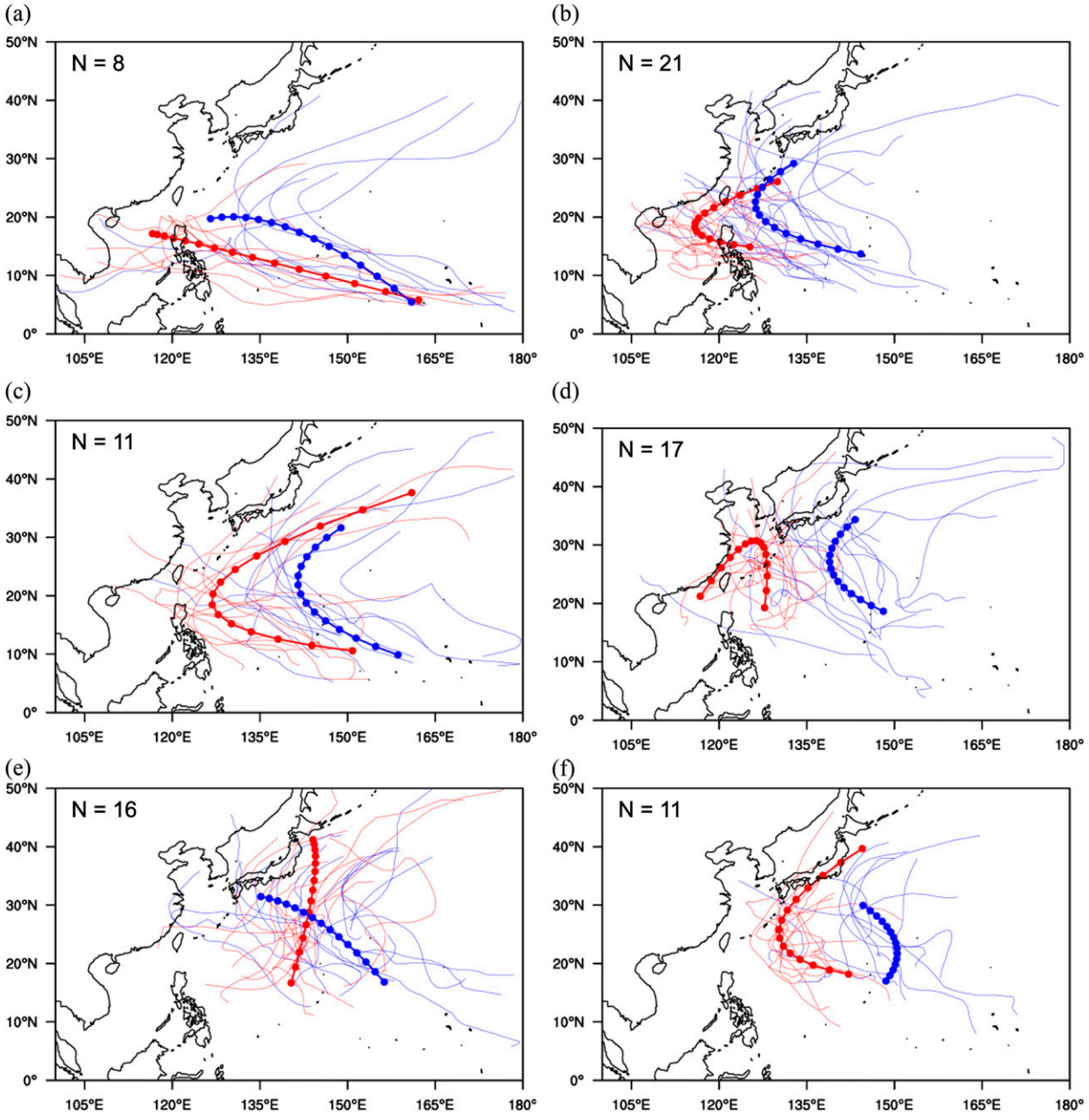

FIG. 5. Six types of clustered binary TCs with the number of cases for each type. The thin red and blue lines in each figure indicate the individual TC of the western and eastern TC in each group, respectively. The thick solid lines indicate the regressed tracks of individual TCs.

b. *Effects of environmental conditions on the clustered tracks*

To investigate the effects of the environmental flow on binary TCs during the evolution of binary TCs in each type, composite analysis is performed by using eight binary TC pairs belonging to each type with respect to three stages: initial, middle, and final stages. The initial and final stages are defined as the genesis and extinction time of the TC that forms first and disappears later between the two TCs, respectively. The middle stage is defined as the center time point between the times for the initial and final stages. The composites of the geopotential height at 500 hPa, steering flow, and relative vorticity at 850 hPa for the three stages of each type are shown in Fig. 6.

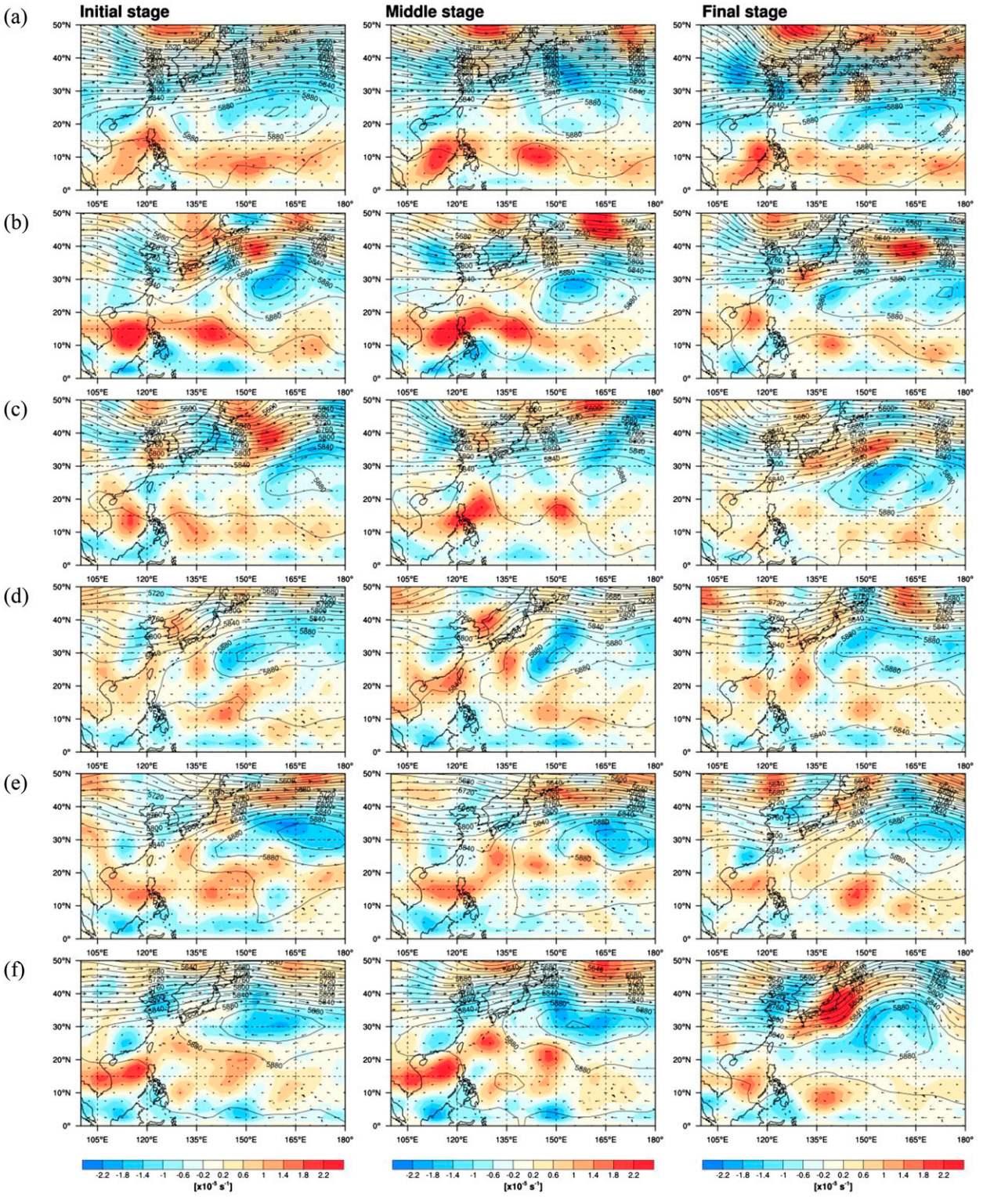

FIG. 6. Composites of geopotential height at 500 hPa (contour), environmental steering flow (vector), and relative vorticity at 850 hPa (shading) at the (left) initial, (middle) middle, and (right) final stages for eight binary TCs of type (a) A, (b) B, (c) C, (d) D, (e) E, and (f) F. Definitions of the initial, middle, and final stages are provided in the text. The contour interval in each figure is 20 m.

In type A (Fig. 6a), the strong North Pacific high is present in the wide region of the WNP in the initial stage and the western boundary of the 5880-gpm line reaches to 130°E. A strong westward steering flow is formed to the south of the North Pacific high. Although the strength of the North Pacific high is slightly weakened in the middle stage, it expands westward again in the final stage. The strong positive low-level vorticity is present along the low-latitude region (0°–10°N) and this feature is retained from the initial to the final stage. These environmental conditions are likely to induce continuous westward movements of the two TCs, as shown in Fig. 5a. Compared to type A, the strength of the North Pacific high decreases and the westward steering flow at the low latitude is also weakened in type B (Fig. 6b), although it expands westward in the final stage. Therefore, the two TCs recurve rather than moving westward continuously. Similar to type A, a positive low-level vorticity is present at the low latitude (10°–20°N) in type B, except for its slight northward shift. In type C (Fig. 6c), the center of the North Pacific high is shifted more eastward (20°N, 165°E) than that in type B. This result is likely to induce the eastward shift of the recurving locations of the two TCs, in comparison to the regressed tracks of TCs in type B. Similar to types A and B, the positive low-level vorticity at the low latitude is also present in type C, although its strength is generally weaker than those in types A and B.

The North Pacific highs in the initial stage of types D, E, and F are located in the southeastern part of Japan. In types D and E (Figs. 6d and 6f), there is no significant change in the location of the North Pacific high with the time (30°N, 150°E for type D, and 30°N, 170°E for type F). The North Pacific high in type D is likely to affect the recurving movements of the ETC as shown in Fig. 5d, while the complex motions of the WTC is induced by the interaction with the ETC. Although the positive relative vorticity is present to the south and west of the North Pacific high, a significant positive relative vorticity elongated in the west–east direction at a low latitude is not evident, in comparison to types A and B. In type E, because the North Pacific high is located farther to the east than those in the other types, the two TCs interact in the southeastern part of Japan with a small effect from the North Pacific high. The positive relative vorticity is dominant in the southwestern part of the North Pacific high at 15°–30°N. In type F, the spatial patterns of the relative vorticity in the initial and middle stages are generally similar to those in type E, but with slightly higher value. In the geopotential height in type F, the western boundary of the 5880-gpm line reaches the southeastern coast of Japan until the middle stage and then it retreats rapidly eastward in the final stage. Therefore, the WTC recurves by the influence of the North Pacific high until the middle stage and the ETC recurves or moves northwestward during the rapid retreat of the North Pacific high, as shown in Fig. 5f.

5. Summary and conclusions

In this study, the statistical and dynamical characteristics of binary tropical cyclones observed in the WNP for 62 years (1951–2012) are investigated. To detect the binary TCs, a new criterion that is slightly modified from previous studies is defined as follows: the two TCs coexisted within 1600 km of each other for more than 24 h with a maximum wind speed greater than 17.2 m s^{-1}. Based on the present definition of a binary TC, 98 binary TC systems are selected. The annual average of occurrence frequency is 1.58 between 1951 and 2012 in the WNP, which is slightly larger than that obtained in B70 (1.47) and DN83 (1.43), but less than half of that obtained in W11 (3.58). The occurrence frequency shows significant year-to-year variation with two periods of strong activity in the mid-1960s and early 1990s. Most of the binary TCs occurred between July and September with the maximum number in August, which is consistent with the high activity season of the general TCs in the WNP. However, the correlation coefficient between the number of total TCs and binary TCs is rather small (0.4), although it is statistically significant at a 95% confidence level. The spectral analysis in the time series of the number of TCs shows dominant periods at 3.6 and 2.5 years for total TCs and 5.6 years for binary TCs. For total TCs, there is no significant difference in the occurrence numbers between the different phases of the ENSO (El Niño and La Niña) and the QBO (easterly QBO and westerly QBO), while more TCs occurred during strong monsoon years with a 90% statistical significance. On the contrary, more binary TCs occurred in the El Niño (23%), easterly phase QBO (31%), and strong monsoon years (34%) than in the La Niña, westerly phase QBO, and weak monsoon years, although their differences are not statistically significant due to the small sample size.

The spatial distribution of binary TCs is different from that of total TCs. The maximum track density of total TCs is located to the east and west of the Philippines, while the maximum track density of binary TCs is located to the east and north of the maximum total TCs. This difference in track density is likely due to the genesis locations and environmental conditions. In comparison with total TCs, the region for higher genesis density of binary TCs shifts eastward and is concentrated in a narrow region.

Environmental conditions for binary and nonbinary TCs at the formation time are investigated using

composite analysis. In comparison with nonbinary TCs, the North Pacific high for binary TCs retreats and the significant poleward steering flow is shown near 20°N. This steering flow prevents westward movements of binary TCs and keeps TCs over the ocean. The vertical wind shear is weaker for binary TCs in the midlatitude region of the WNP than for nonbinary TCs. Although a short period of SST data (1982–2012) is used for compositing, it is found that SST for binary TCs to the north of 20°N is significantly larger than that for nonbinary TCs. These three environmental conditions—poleward steering flow, weaker vertical wind shear, and warmer SST—result in a longer lifetime for TCs by maintaining TCs over the ocean longer, which can provide enough humidity to sustain the TCs under weak vertical shear and warm SST conditions. Considering that the criteria for detecting binary TCs include the intensities of the two TCs, their separation distance, and their coexistence time, TCs with longer lifetimes have more opportunities to become part of a binary system.

Six representative tracks of binary TCs are obtained by using clustering analysis and the effects of environmental conditions on the clustered tracks are investigated. The tracks of each type show distinct characteristics and the TCs in types A, B, and C are formed at lower latitude than those in types D, E, and F. The regressed tracks of types A, B, and C are more typical tracks of TCs in the WNP, such as continuous westward movements or recurving motions, while those in types D, E, and F show various and unusual tracks moving near the Korean Peninsula and Japan. The impacts of environmental conditions during the evolution of each type of binary TC are investigated using the composites of the geopotential height at 500 hPa, steering flow, and relative vorticity at 850 hPa at the initial, middle, and final stages. In the evolution of binary TCs, the movements of the two TCs are strongly influenced by the strength and location of the North Pacific high, which has a strong influence on the steering flow. The spatial distributions of the composites for the relative vorticity at 850 hPa showed different features with respect to the clustered types.

Although this study examined the environmental conditions that may be favorable for binary TCs, deducing the major factors that determine the occurrence of binary TCs among general TCs is not straightforward. In addition, this study takes only the SST into consideration for the thermodynamic variable, but other thermodynamic variables, such as moisture, convective activity, and temperature in the upper-troposphere and lower-stratosphere regions (Emanuel et al. 2013), may be important for binary TC formation and evolution, which remains a topic for future study.

Acknowledgments. This study was supported by the National Research Foundation of Korea (NRF) grant funded by the Korean government (MEST) (Grant 2013R1A2A2A01014644).

REFERENCES

Brand, S., 1970: Interaction of binary tropical cyclones of the western North Pacific Ocean. *J. Appl. Meteor.,* **9,** 433–441, doi:10.1175/1520-0450(1970)009<0433:IOBTCO>2.0.CO;2.

Camargo, S. J., A. W. Robertson, S. J. Gaffney, P. Smyth, and M. Ghil, 2007: Cluster analysis of typhoon tracks. Part I: General properties. *J. Climate,* **20,** 3635–3653, doi:10.1175/JCLI4188.1.

Carr, L. E., III, and R. L. Elsberry, 1998: Objective diagnosis of binary tropical cyclone interactions for the western North Pacific basin. *Mon. Wea. Rev.,* **126,** 1734–1740, doi:10.1175/1520-0493(1998)126<1734:ODOBTC>2.0.CO;2.

——, M. A. Boother, and R. L. Elsberry, 1997: Observational evidence for alternate modes of track-altering binary tropical cyclone scenarios. *Mon. Wea. Rev.,* **125,** 2094–2111, doi:10.1175/1520-0493(1997)125<2094:OEFAMO>2.0.CO;2.

Chan, J. C. L., and W. M. Gray, 1982: Tropical cyclone movement and surrounding flow relationships. *Mon. Wea. Rev.,* **110,** 1354–1374, doi:10.1175/1520-0493(1982)110<1354:TCMASF>2.0.CO;2.

Chand, S. S., and K. J. E. Walsh, 2009: Tropical cyclone activity in the Fiji region: Spatial patterns and relationship to large-scale circulation. *J. Climate,* **22,** 3877–3893, doi:10.1175/2009JCLI2880.1.

Chang, S. W.-J., 1983: A numerical study of the interaction between two tropical cyclones. *Mon. Wea. Rev.,* **111,** 1806–1817, doi:10.1175/1520-0493(1983)111<1806:ANSOTI>2.0.CO;2.

DeMaria, M., 1996: The effect of vertical shear on tropical cyclone intensity change. *J. Atmos. Sci.,* **53,** 2076–2087, doi:10.1175/1520-0469(1996)053<2076:TEOVSO>2.0.CO;2.

——, and J. C. L. Chan, 1984: Comments on ''A numerical study of the interactions between two tropical cyclones.'' *Mon. Wea. Rev.,* **112,** 1643–1645, doi:10.1175/1520-0493(1984)112<1643:CONSOT>2.0.CO;2.

Dong, K., and C. J. Neumann, 1983: On the relative motion of binary tropical cyclones. *Mon. Wea. Rev.,* **111,** 945–953, doi:10.1175/1520-0493(1983)111<0945:OTRMOB>2.0.CO;2.

Dritschel, D. G., and D. W. Waugh, 1992: Quantification of the inelastic interaction of unequal vortices in two-dimensional vortex dynamics. *Phys. Fluids,* **4A,** 1737–1744, doi:10.1063/1.858394.

Emanuel, K. A., 1988: The maximum intensity of tropical cyclones. *J. Atmos. Sci.,* **45,** 1143–1155, doi:10.1175/1520-0469(1988)045<1143:TMIOH>2.0.CO;2.

——, S. Solomon, D. Folini, S. Davis, and C. Cagnazzo, 2013: Influence of tropical tropopause layer cooling on Atlantic hurricane activity. *J. Climate,* **26,** 2288–2301, doi:10.1175/JCLI-D-12-00242.1.

Falkovich, A. I., A. P. Khan, and I. Ginis, 1995: Motion and evolution of binary tropical cyclones in a coupled atmosphere–ocean numerical model. *Mon. Wea. Rev.,* **123,** 1345–1363, doi:10.1175/1520-0493(1995)123<1345:MAEOBT>2.0.CO;2.

Frank, W. M., and E. A. Ritchie, 2001: Effects of vertical wind shear on the intensity and structure of numerically simulated hurricanes. *Mon. Wea. Rev.,* **129,** 2249–2269, doi:10.1175/1520-0493(2001)129<2249:EOVWSO>2.0.CO;2.

Fujiwhara, S., 1921: The mutual tendency towards symmetry of motion and its application as a principle in meteorology.

Quart. J. Roy. Meteor. Soc., **47,** 287–293, doi:10.1002/qj.49704720010.

——, 1923: On the growth and decay of vortical systems. *Quart. J. Roy. Meteor. Soc.,* **49,** 75–104, doi:10.1002/qj.49704920602.

——, 1931: Short note on the behavior of two vortices. *Proc. Phys. Math. Soc. Japan. Ser. 3,* **13,** 106–110.

Gaffney, S., 2004: Probabilistic curve-aligned clustering and prediction with mixture models. Ph.D. dissertation, University of California, Irvine, 281 pp.

George, J. E., and W. M. Gray, 1976: Tropical cyclone motion and surrounding parameter relationships. *J. Appl. Meteor.,* **15,** 1252–1264, doi:10.1175/1520-0450(1976)015<1252:TCMASP>2.0.CO;2.

Ho, C.-H., H.-S. Kim, J.-H. Jeong, and S.-W. Son, 2009: Influence of stratospheric quasi-biennial oscillation on tropical cyclone tracks in the western North Pacific. *Geophys. Res. Lett.,* **36,** L06702, doi:10.1029/2009GL037163.

Huesmann, A. S., and M. H. Hitchman, 2001: The stratospheric quasi-biennial oscillation in the NCEP reanalyses: Climatological structures. *J. Geophys. Res.,* **106,** 11 859–11 874, doi:10.1029/2001JD900031.

Jang, W., and H.-Y. Chun, 2013: The effects of topography on the evolution of Typhoon Saomai (2006) under the influence of Tropical Storm Bopha (2006). *Mon. Wea. Rev.,* **141,** 468–489, doi:10.1175/MWR-D-11-00241.1.

Jarrell, J., S. Brand, and D. S. Nicklin, 1978: An analysis of western North Pacific tropical cyclone forecast errors. *Mon. Wea. Rev.,* **106,** 925–937, doi:10.1175/1520-0493(1978)106<0925:AAOWNP>2.0.CO;2.

Kalnay, E., and Coauthors, 1996: The NCEP/NCAR 40-Year Reanalysis Project. *Bull. Amer. Meteor. Soc.,* **77,** 437–471, doi:10.1175/1520-0477(1996)077<0437:TNYRP>2.0.CO;2.

Kanamitsu, M., W. Ebisuzaki, J. Woollen, S.-K. Yang, J. J. Hnilo, M. Fiorino, and G. L. Potter, 2002: NCEP–DOE AMIP-II Reanalysis (R-2). *Bull. Amer. Meteor. Soc.,* **83,** 1631–1643, doi:10.1175/BAMS-83-11-1631.

Khain, A., I. Ginis, A. Falkovich, and M. Frumin, 2000: Interaction of binary tropical cyclones in a coupled tropical cyclone-ocean model. *J. Geophys. Res.,* **105,** 22 337–22 354, doi:10.1029/2000JD900268.

Kleinbaum, D. G., L. L. Kupper, K. E. Muller, and A. Nizam, 1997: *Applied Regression Analysis and Multivariable Methods.* Duxbury Press, 816 pp.

Kuo, H.-C., G. T.-J. Chen, and C.-H. Lin, 2000: Merger of tropical cyclones Zeb and Alex. *Mon. Wea. Rev.,* **128,** 2967–2975, doi:10.1175/1520-0493(2000)128<2967:MOTCZA>2.0.CO;2.

Lander, M. A., 1994: An exploratory analysis of the relationship between tropical storm formation in the western North Pacific and ENSO. *Mon. Wea. Rev.,* **122,** 636–651, doi:10.1175/1520-0493(1994)122<0636:AEAOTR>2.0.CO;2.

——, and G. J. Holland, 1993: On the interaction of tropical-cyclone-scale vortices. I: Observation. *Quart. J. Roy. Meteor. Soc.,* **119,** 1347–1361, doi:10.1002/qj.49711951406.

Lighthill, J., G. Holland, W. M. Gray, C. Landsea, G. Craig, J. Evans, Y. Kurihara, and C. Guard, 1994: Global climate change and tropical cyclones. *Bull. Amer. Meteor. Soc.,* **75,** 2147–2157.

McBride, J. L., 1995: Tropical cyclone formation. *Global Perspectives on Tropical Cyclones,* WMO/TD-693, J. C. L. Chan and J. D. Kepert, Eds., World Meteorological Organization, 63–105.

——, and R. M. Zehr, 1981: Observational analysis of tropical cyclone formation. Part II: Comparison of nondeveloping versus developing systems. *J. Atmos. Sci.,* **38,** 1132–1151, doi:10.1175/1520-0469(1981)038<1132:OAOTCF>2.0.CO;2.

Merrill, R. T., 1988: Characteristics of the upper-tropospheric environmental flow around hurricanes. *J. Atmos. Sci.,* **45,** 1665–1677, doi:10.1175/1520-0469(1988)045<1665:COTUTE>2.0.CO;2.

Neumann, C. J., 1981: Trends in forecasting the tracks of Atlantic tropical cyclones. *Bull. Amer. Meteor. Soc.,* **62,** 1473–1485.

Pokhil, A. E., I. G. Sitnikov, V. A. Zlenko, and I. V. Polyakova, 1990: Numerical experiments on investigation of atmospheric vortices. *Meteor. Gidrol.,* **4,** 21–28.

Prieto, R., B. D. McNoldy, S. R. Fulton, and W. H. Schubert, 2003: A classification of binary tropical cyclone–like vortex interactions. *Mon. Wea. Rev.,* **131,** 2656–2666, doi:10.1175/1520-0493(2003)131<2656:ACOBTC>2.0.CO;2.

Reynolds, R. W., T. M. Smith, C. Liu, D. B. Chelton, K. S. Casey, and M. G. Schlax, 2007: Daily high-resolution-blended analyses for sea surface temperature. *J. Climate,* **20,** 5473–5496, doi:10.1175/2007JCLI1824.1.

Ritchie, E. A., and G. J. Holland, 1993: On the interaction of tropical-cyclone-scale vortices. II: Discrete vortex patches. *Quart. J. Roy. Meteor. Soc.,* **119,** 1363–1379, doi:10.1002/qj.49711951407.

Shin, S.-E., J.-Y. Han, and J.-J. Baik, 2006: On the critical separation distance of binary vortices in a nondivergent barotropic atmosphere. *J. Meteor. Soc. Japan,* **84,** 853–869, doi:10.2151/jmsj.84.853.

Wang, B., and Z. Fan, 1999: Choice of South Asian summer monsoon indices. *Bull. Amer. Meteor. Soc.,* **80,** 629–638, doi:10.1175/1520-0477(1999)080<0629:COSASM>2.0.CO;2.

——, R. Wu, and K. M. Lau, 2001: Interannual variability of Asian summer monsoon: Contrast between the Indian and western North Pacific–East Asian monsoons. *J. Climate,* **14,** 4073–4090, doi:10.1175/1520-0442(2001)014<4073:IVOTAS>2.0.CO;2.

Wu, C.-C., T.-S. Huang, W.-P. Huang, and K.-H. Chou, 2003: A new look at the binary interaction: Potential vorticity diagnosis of the unusual southward movement of Tropical Storm Bopha (2000) and its interaction with Supertyphoon Saomai (2000). *Mon. Wea. Rev.,* **131,** 1289–1300, doi:10.1175/1520-0493(2003)131<1289:ANLATB>2.0.CO;2.

Wu, X., J.-F. Fei, X.-G. Huang, X.-P. Cheng, and J.-Q. Ren, 2011: Statistical classification and characteristics analysis of binary tropical cyclones over the western North Pacific Ocean. *J. Trop. Meteor.,* **17,** 335–344.

——, ——, ——, X. Zhang, X.-P. Cheng, and J.-Q. Ren, 2012: A numerical study of the interaction between two simultaneous storms: Goni and Morakot in September 2009. *Adv. Atmos. Sci.,* **29,** 561–574, doi:10.1007/s00376-011-1014-7.

Yang, C.-C., C.-C. Wu, K.-H. Chou, and C.-Y. Lee, 2008: Binary interaction between Typhoons Fengshen (2002) and Fungwong (2002) based on the potential vorticity diagnosis. *Mon. Wea. Rev.,* **136,** 4593–4611, doi:10.1175/2008MWR2496.1.